IOSR Journal of Applied Chemistry (IOSR-JAC)
e-ISSN: 2278-5736.Volume 16, Issue 9 Ser. I (September 2023), PP 15-24
www.iosrjournals.org

Dft Study Of The Physicochemical Properties Of Derivatives Of An Anticancer Molecule: Suberoylanilide Hydroxamic Acid

Konate Bibata[1,3], Kouman Koffi Charles[2],
Dembele Georges Stéphane[1,3,*], Ouattara Ladji Bafétégué[1],
Soro Doh[1], Konate Fandia[1], Tuo Nanou Tiéba[1],
Koné Mamadou Guy-Richard[1,3,4] And Ziao Nahossé[1,3]

[1]*laboratoire De Thermodynamique Et De Physico-Chimie Du Milieu, Université Nangui Abrogoua, Abidjan, Côte-D'ivoire*
[2]*laboratoire De Physique Fondamentale Et Appliquée, Ufr Sfa, Université Nangui Abrogoua, Abidjan, Côte-D'ivoire*
[3]*groupe Ivoirien De Recherches En Modélisation Des Maladies (Gir2m), Université Nangui Abrogoua, Abidjan, Côte-D'ivoire*
[4]*e2s Uppa, Cnrs, Iprem, Université De Pau Et Des Pays De L'adour, 64053 Pau, France*

Abstract
SAHA or vorinostat is a new drug used in the management of cutaneous T-cell lymphoma when the disease persists, worsens or recurs during or after treatment with other drugs. It is an effective, well-tolerated treatment for this type of cancer. In addition to cutaneous T-cell lymphoma, the role of vorinostat in other types of cancer is being studied both as monotherapy and in combination therapy. While studies on the SAHA attachment and linker groups are well known, the role of the linker remains little studied today. Could the carbon number present in the linker improve the biological activity of SAHA? This is the question we set out to answer.
To this end, we investigated the carbon chain length of SAHA by studying new compounds with less carbon (LESS) on the one hand, and compounds with more carbon (MORE) than SAHA on the other. This theoretical study was carried out while retaining the other two groups and modifying the number of carbons in the carbon chain. All calculations were performed at the B3LYP/6-311G(d,p) level of theory. For these SAHA derivatives, the standard thermodynamic formation quantities show that these new compounds can exist and have good stability. Reactivity indices were also used to identify the zinc-binding sites of these derivatives. Finally, activity prediction was carried out using the HDAC1 and HDAC7 models established in a previous work.

Date of Submission: 08-09-2023 Date of Acceptance: 18-09-2023

I. INTRODUCTION

Histone deacetylases (HDACs) have been identified as one of the main causes of tumorigenesis [1]. HDACs have thus become very important targets in the fight against cancer, as they are aberrantly found in different types of cancer cells [2]. Inhibition of HDACs has proved effective in the treatment of cancer, as this strategy leads cancer cells to cell death. To date, 18 human HDACs have been identified and grouped into four different classes. However, the search is on for new drugs capable of inhibiting these HDACs. Indeed, suberoylanilide hydroxamic acid (SAHA) has been approved as an effective inhibitor of histone deacetylases, capable of binding the zinc ion present in the active site of HDAC enzymes [3]. SAHA or Vorinostat is a molecule belonging to the hydroxamic acid family. Hydroxamic acids are a family of chemical compounds with multiple biological activities. They are effective and selective inhibitors of a large number of enzymes, such as ureases [4], matrix metalloproteinases [5], histone deacetylases [6], etc. The detailed role of hydroxamic acid derivatives as enzyme inhibitors has been well described by Muri et al [7]. They have been developed as drugs against all those diseases that can arise through over-activation of these enzymes. As well as acting as enzyme inhibitors, hydroxamic acids have also been described as acting against cancer [8], malaria, tuberculosis and fungi [9], HIV [10], Alzheimer's disease and cardiovascular disorders [11]. All these biological activities of hydroxamic acids are due to their structure, which enables them to form multiple hydrogen bonds with the enzyme. They are also used as metal ion chelators. SAHA is an inhibitor that has been previously evaluated in multiple clinical trials [12]. It inhibits HDAC activity, blocks cell proliferation in culture and inhibits tumor growth in various animal models.

The efficacy of vorinostat in patients with cutaneous T-cell lymphoma is well established, and its efficacy and safety in other types of cancer as part of combination therapy is the subject of numerous studies. In earlier work, Soro et al [13] showed that SAHA binds appropriately to the HDAC1 and HDAC7 enzymes, which are overexpressed in many types of cancer. The aim of this work is to study the effect of the carbon chain size of SAHA (linker) on the chemical reactivity, thermodynamic formation parameters and biological activity of its derivatives.

II. MATERIALS AND CALCULATION METHODS

Calculation software and compounds used

Calculation software

Molecular geometries were optimized at the B3LYP/6-311G(d,p) level of theory, using the Gaussian09 program [14]. Molecular models were built using the graphical interface of the GaussView program [15].

ChemDraw Ultra 12.0 [16] is a comprehensive drawing tool that lets you create scientifically intelligent, ready-to-use drawings. It enabled us to make a 2D representation of our molecules.

Compounds used

The six (06)-carbon carbon chain (Linker) of suberoylanilide acid (SAHA), which separates the attachment group from the linking group, was varied to obtain the eleven derivatives to be studied. The LESS are obtained by decreasing the number of linker carbons coded LESS0, LESS1, LESS2, LESS3, LESS4 and LESS5. Increasing the number produces MOREs, including MORE1, MORE2, MORE3, MORE4 and MORE5. The molecular structures of these compounds are given in Table 1.

Table 1: Structures of the compounds studied.

Codes	Structures
LESS0	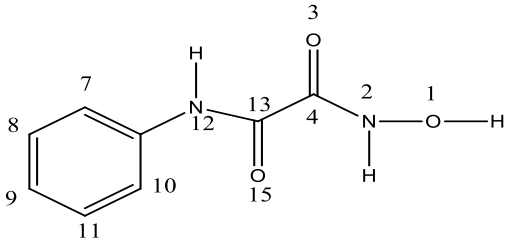
LESS1	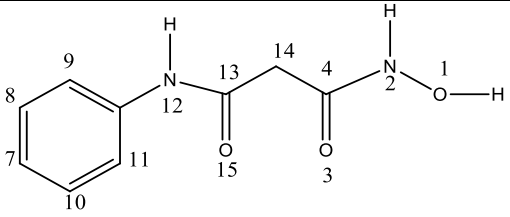
LESS2	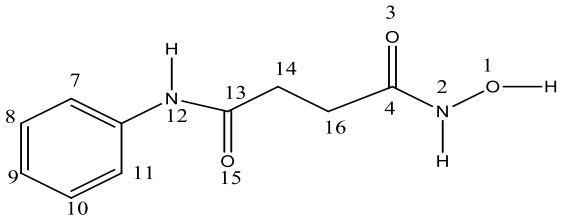
LESS3	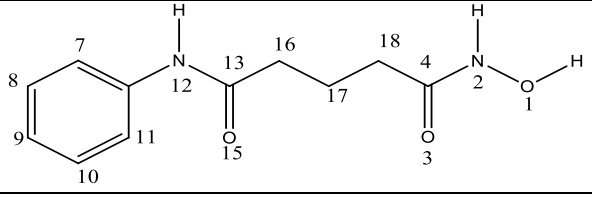

4	LESS	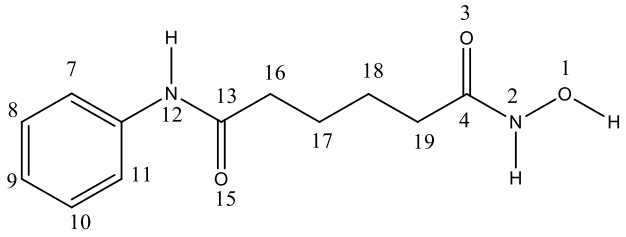
5	LESS	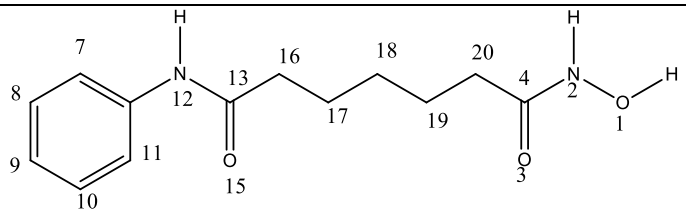
E1	MOR	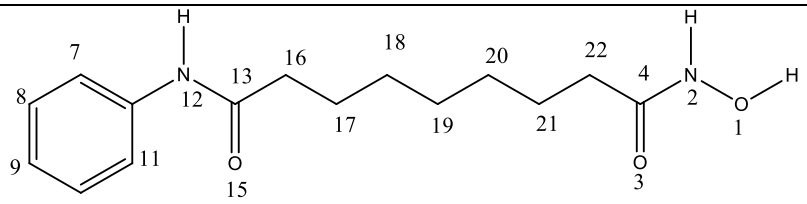
E2	MOR	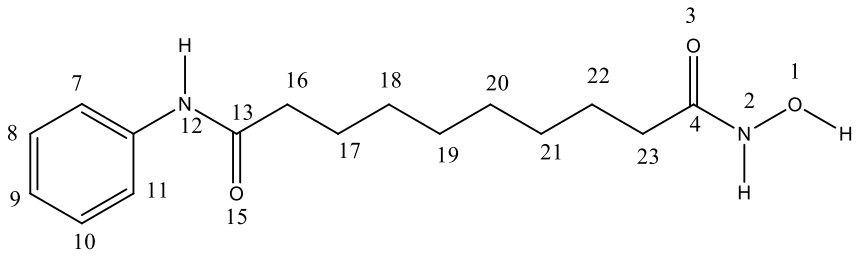
E3	MOR	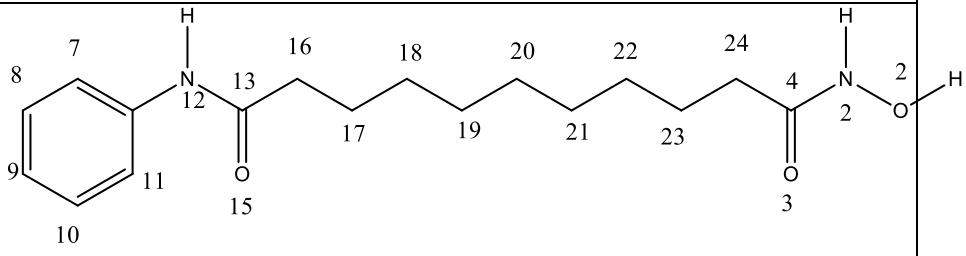
E4	MOR	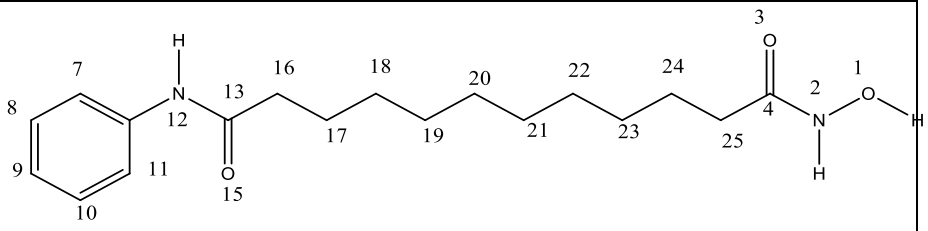
E5	MOR	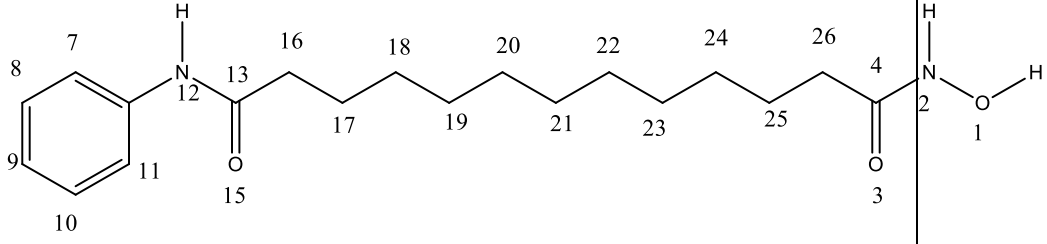

Thermodynamic formation quantities

The standard formation quantity of a body, $\Delta_f z^0$, is the variation in z during the formation reaction of one mole of this body from the simple pure bodies of which it is composed, under standard conditions of temperature and pressure (T=298.15; P=1 atm). The results of quantum calculations and the use of experimental data in the form of reference thermodynamic tables [16] enable us to determine standard values for the enthalpy, entropy and free enthalpy of formation of the product at 298.15 K at 1 atm. The enthalpy of formation of a molecule is calculated according to the following relationship [17]:

$$\Delta_f H^0(M, 298K) = \Delta_f H^0(M, 0K) + H_M^0(298K) - H_M^0(0K)$$

$$\Delta_f H^0(M, 0K) = \sum_{Atomes} n_x \Delta_f H^0(X, 0K) - \sum D_0(M)$$

n_x : The number of atoms of species X in molecule M.

$\Delta_f H^0(X, 0K)$: is an experimental value corresponding to the heat of formation of atom X at 0 K.

$\sum D_0(M)$: is the atomization energy of the M molecule.

This energy comes from the decomposition of one mole of the molecule into its constituent atoms. The calculation of $\sum D_0(M)$ is calculated from the latter's internal energies at 0 K (ZPVE) according to the following relationship:

$$\sum D_0(M) = \sum_{Atomes} n_x E_{él}(X) - [E_{él}(M) + ZPVE(M)]$$

The relationship used for the determination is:

$$\Delta_f S^0(M, 298K) = S^0(M, 298K) - \sum n_x S^0(X, 298K)$$

The standard free enthalpy of formation at 25°C is calculated according to the following equation:

$$\Delta_f G^0(M, 298K) = \Delta_f H^0(M, 298K) - 298{,}15 \times \Delta_f S^0(M, 298K)$$

Global reactivity indices

Calculations included chemical potential (μ), hardness (η), softness (S) and electrophilicity index (ω) according to the Koopmans approximation [17] using the energies of the HOMO and LUMO boundary molecular orbitals according to the relations [18, 19]:

$$\mu = \frac{E_{HOMO} + E_{LUMO}}{2} = -\chi$$

$$\eta = \frac{E_{LUMO} - E_{HOMO}}{2} = \frac{1}{S}$$

$$\omega = \frac{\mu^2}{2\eta}$$

Local reactivity indices

Determination of the reactivity sites of the various molecules was based on Fukui indices calculated using the finite difference approximation method: [20, 21].

$$f_k^+ = q_k(N+1) - q_k(N)$$

$$f_k^- = \mathrm{q_k(N) - q_k(N-1)}$$

$$\mathrm{f_k^0 = \frac{1}{2}[f_k^+ + f_k^-] = \frac{1}{2}[q_k(N+1) - q_k(N-1)]}$$

where $q_k(N)$, $q_k(N-1)$, $q_k(N+1)$ are the net atomic charges of the $k^{ième}$ site in the neutral, cationic and anionic forms, respectively, of each molecule. f_k^+ and f_k^- are used to identify, in order, the most favorable site for nucleophilic and electrophilic attack.

To distinguish the case of electron, gain from electron loss, two Fukui functions have been proposed. The first f_k^+ is the electron density response to electron gain at constant external potential. It will therefore give information on the most electrophilic sites vis- à- vis a nucleophilic attack. The second f_k^- is the response to electron loss at a fixed potential. This provides information on the most nucleophilic sites for electrophilic attack. A third function, $\mathrm{f_k^0}$, describes radical attack.

Prediction of inhibitory activities of SAHA derivatives

A study by Soro et al [13] on the structure and activity of hydroxamic acids led to the development of two models: HDAC 1 and HDAC 7.

The HDAC 1 model

A study carried out on a set of twenty-one (21) hydroxamic acids, on a test set of ten (10) other molecules, enabled Soro et al [13] to develop a relationship between hydroxamic acid structure and activity. Implementation of this model requires a number of geometric descriptors: valence angles (O=C-N) and (H-N-O) and bond length d(C=O).

$$IC_{50}^{Théo} = 8875 - 6751 * \boldsymbol{d}(\boldsymbol{C=O}) - 29.76933 * \boldsymbol{\alpha}^{\circ}(\boldsymbol{O=C-N}) + 26.63001 * \boldsymbol{\alpha}^{\circ}(\boldsymbol{H-N-O})$$

Significance of Model file: F=575,56

The cross-correlation coefficient: Q^2_{cv}=0,968>0,9

Model performance: R^2- Q^2_{cv}<0,3

The HDAC 7 model

This HDAC 7 model is based on nineteen (19) observables that are functions of three (03) descriptors, including electron affinity (ΔE), vibrational frequency V(0-H) and V(N-H).

$$\mathrm{pIC}_{50}^{\mathrm{Théo}}(\mathrm{HDAC7}) = -902{,}89167 - 1{,}16813 * \mathbf{AE} + 0{,}35349 * \mathbf{V(O-H)} - 0{,}09615 * \mathbf{V(N-H)}$$

Significance of Model file: F=84,99

The cross-correlation coefficient : Q^2_{cv}=0,95>0,9

The linear correlation coefficient : R^2=0,9659

Model performance : R^2- Q^2_{cv}<0,3

III. RESULTS AND DISCUSSION

Analysis of thermodynamic parameters of formation

The standard thermodynamic parameters of formation, namely enthalpy of formation $\Delta_f \boldsymbol{H}^{\circ}_{\boldsymbol{298}}$, entropy of formation $\Delta_f \boldsymbol{S}^{\circ}_{\boldsymbol{298}}$ and free enthalpy of formation $\Delta_f \boldsymbol{G}^{\circ}_{\boldsymbol{298}}$, were also determined. The values of the thermodynamic parameters are recorded in Table 2.

Table 2: Thermodynamic formation quantities for the eleven (11) molecules optimized at B3LYP/6-311G (d, p).

Compounds	$\Delta_f H^{\circ}_{298}$ (kcal/mol)	$\Delta_f S^{\circ}_{298}$°(Cal/mol.K)	$\Delta_f G^{\circ}_{298}$ (kcal/mol)
LESS 0	-1350.129	-0.523	-1194.104
LESS 1	-1433.329	-0.632	-1244.909
LESS 2	-1516.294	-0.710	-1304.641
LESS 3	-1597.663	-0.792	-1361.550
LESS 4	-1683.517	-0.871	-1423.845
LESS 5	-1765.060	-0.951	-1481.390
MORE 1	-1934.545	-1.114	-1602.354
MORE 2	-2017.345	-1.195	-1661.135
MORE 3	-2099.964	-1.273	-1720.345
MORE 4	-2142.579	-1.405	-1723.759
MORE 5	-2252.691	-1.438	-1823.917

Analysis of this table shows that all enthalpy, free enthalpy and entropy of formation variation values are negative ($\Delta_f \boldsymbol{H}^{\circ}_{\boldsymbol{298}}$<0, $\Delta_f \boldsymbol{G}^{\circ}_{\boldsymbol{298}}$<0 and $\Delta_f \boldsymbol{S}^{\circ}_{\boldsymbol{298}}$<0). These results show the stability of formation of the eleven (11) derivative compounds. Overall the formation of SAHA derivatives is possible and occurs spontaneously, exothermically with a decrease in disorder at these experimental conditions.

Border molecular orbital analysis

The energy parameters for stability and reactivity information, obtained from frontier orbital energies, are shown in Table 3.

Table 3: Molecular boundary orbital energy values and differences for eleven compounds

Compounds	E_{HO}(ev)	E_{BV}(ev)	ΔE_{gap}(ev)
LESS0	-6.544	-1.735	**4.809**
LESS1	-6.503	-1.099	5.404
LESS2	-6.358	-0.728	5.631
LESS3	-6.333	-0.710	5.623
LESS4	-6.285	-0.639	5.646
LESS5	-6.263	-0.615	5.648

MORE1	-6.221	-0.570	5.651
MORE2	-6.184	-0.531	5.653
MORE3	-6.213	-0.560	5.653
MORE4	-6.509	-0.489	**6.020**
MORE5	-6.200	-0.548	5.652
SAHA	-6.229	-0.574	**5.656**

These results show that the LESS0 molecule, with the smallest energy gap (ΔEgap=4.809eV) is the most reactive, while the MORE4 molecule with the largest energy gap (6.020eV) is the most stable of the ten (10) molecules studied. The order of increasing energy gap is as follows:

LESS0 < LESS1 < LESS3 < LESS2 < LESS4 < LESS5 < MORE1 < MORE5 < MORE2 < MORE3< MORE4

Compared with SAHA, LESS0 is the most reactive because SAHA has a higher energy gap.

Global reactivity descriptors

The conceptual DFT descriptors determined have contributed in many ways to understanding the structure of molecules and their reactivity. The reactivity parameters examined in this series of compounds are: chemical potential (μ), hardness (η), softness (S) and electrophilicity index (ω). The calculated values of the said parameters are reported in Table 4.

Table 4: Summary of global reactivity descriptors at B3LYP/6-311G (d, p) calculation level.

Compounds	**χ(eV)**	**μ(eV)**	**η(eV)**	**Ꞷ(eV)**	**S(eV)**
LESS0	**4.151**	**-4.151**	4.235	**2.035**	0.236
LESS1	3.802	-3.802	4.390	1.646	0.228
LESS2	3.552	-3.552	4.472	1.411	0.224
LESS3	3.603	-3.603	4.447	1.460	0.225
LESS4	3.474	-3.474	4.390	1.374	0.228
LESS5	3.512	-3.512	4.398	1.403	0.227
MORE1	3.419	-3.419	4.296	1.361	0.233
MORE2	**0.211**	**-0.211**	**7.581**	**0.003**	**0.132**
MORE3	3.469	-3.469	4.297	1.401	0.233
MORE4	2.904	-2.904	4.910	0.858	0.204
MORE5	3.404	-3.404	**4.226**	1.371	**0.237**
SAHA	**3.426**	**-3.426**	**4.326**	**1.357**	**0.231**

Overall reactivity indices vary according to molecule structure. The electroneutrality values recorded in Table 4 for the eleven molecules allow us to establish the following descending order:

χ(eV) : LESS 0 > LESS 1 > LESS 3 > LESS 2 > LESS 5 > LESS 4 > MORE 3 > MORE 1 > MORE 5 > MORE 4 > MORE 2

It appears that LESS 0, with a much higher electroneutrality value (4.151 eV), is the most electronegative compound. It is therefore the most electron-accepting of all the compounds studied, including SAHA.

With regard to chemical hardness (η) and overall softness (S), we had to establish the following order of decreasing stability

the following descending order of stability:

η(eV): MORE 2 > MORE 4 > LESS 2 > LESS 3 > LESS 5 > LESS 1 > LESS 4 > MORE 3 > MORE 1 > LESS 0 >MORE 5

Hardness increases with molecule stability, while softness increases with molecule reactivity.

reactivity of the molecule. So, the harder a molecule, the more stable and less reactive it is.

It's clear that MORE5 has the lowest overall hardness (η= 4.226 eV) and the highest softness (S= 0.237 eV). As a result, MORE5 is the most reactive of all the molecules studied. SAHA remains less reactive than MORE5, so carbon chain lengthening has a positive influence on SAHA's reactivity.

Table 4 also shows the order of decay of the overall electrophilicity index:

Ꞷ(eV) : LESS 0 > LESS 1 > LESS 3 > LESS 2 > LESS 5 > MORE 3 > LESS 4 > MORE 5 > MORE 1 > MORE 4 > MORE 2

The electrophilic index value of the LESS 0 compound (GƟ= 2.035 eV) indicates that it is more electrophilic than SAHA.

Local reactivity descriptors

The Fukui indices used to characterize the electrophilic and nucleophilic attack sites localized for each molecule studied are determined and presented. Only the heavy atoms making up the compounds are concerned by this study. As the aim of this study is to determine the atom(s) that can bind the zinc ion, we will present only those atoms of significant interest to our study. The reference being vorinostat, we present the table containing the theoretical values of its Fukui indices.

Local Fukui index values, calculated at the B3LYP/6-311G (d, p) level, using natural population analysis (NPA) for SAHA.

Table 5: Local reactivity index values for SAHA

SAHA			
	f_k^+	f_k^-	f_k^0
O1	0.031	0.101	0.066
N2	-0.015	0.111	0.048
O3	**0.122**	0.000	0.061
C4	0.104	-0.026	0.039
O15	0.027	**0.123**	0.075
C13	0.100	0.005	0.052
N12	-0.002	0.082	0.040

Analysis of the data in Table 5 indicates that the highest nucleophilic Fukui value is obtained with the O15 atom, which is the preferred center for all electrophilic attacks, while the highest electrophilic Fukui value is obtained with the O3 atom. However, the latter will be the most likely site for nucleophilic attacks.

Table 6: Local reactivity index values for SAHA LESS derivatives

		O_1	N_2	O_3	C_4	O_{15}	C_{13}	N_{12}
LESS 0	f_k^+	0.058	0.058	0.098	0.075	0.125	0.144	0.013
	f_k^-	0.089	0.059	0.047	-0.012	0.087	0.002	0.087
	f_k^0	0.074	0.058	0.072	0.031	0.106	0.073	0.050
LESS 1		O_1	N_2	O_3	C_4	O_{15}	C_{13}	N_{12}
	f_k^+	0.031	0.017	0.052	0.001	0.109	0.155	-0.007
	f_k^-	-0.031	0.093	0.103	-0.001	0.060	0.001	0.068
	f_k^0	0.066	0.046	0.052	0.024	0.087	0.067	0.039
LESS 2		O_1	N_2	O_3	C_4	O_{15}	C_{13}	N_{12}
	f_k^+	0.030	0.020	0.039	0.049	0.094	0.133	-0.010
	f_k^-	0.101	0.072	0.066	-0.002	0.079	0.001	0.088
	f_k^0	0.066	0.046	0.052	0.024	0.087	0.067	0.039
LESS 3		O_1	N_2	O_3	C_4	O_{15}	C_{13}	N_{12}
	f_k^+	0.030	0.020	0.039	0.049	0.094	0.133	-0.010
	f_k^-	0.101	0.072	0.066	-0.002	0.079	0.001	0.088
	f_k^0	0.066	0.046	0.052	0.024	0.087	0.067	0.039
LESS 4		O_1	N_2	O_3	C_4	O_{15}	C_{13}	N_{12}
	f_k^+	0.030	0.020	0.039	0.049	0.094	0.133	-0.010
	f_k^-	0.101	0.072	0.066	-0.002	0.079	0.001	0.088
	f_k^0	0.066	0.046	0.052	0.024	0.087	0.067	0.039

Analysis of the values in the table shows that oxygen O1 is the most favored site for electrophilic attack among the atoms making up the LESS 0 compound, and that C13 carbon atoms is designated as the nucleophilic attack site in a reaction between LESS0 and the other active HDAC enzymes. The values for LESS1 show that

oxygen O3 is the most likely site for electrophilic attack. In the same approach, the preferred site for nucleophilic electrophilic attack is C13. The C13 atom has the highest electrophilic Fukui number and is therefore the preferred site for nucleophilic attack. The O1 atom has the highest nucleophilic Fukui number, and is the site of electrophilic attack. For the LESS2 compound, the O3 atom is the most favorable site for electrophilic attack. From the point of view of the highest Fukui index f_k^+, nucleophilic attack will occur preferentially on the C13 carbon atom. Compound LESS3 displays the oxygen atom O1 susceptible to electrophilic attack is and that susceptible to nucleophilic attack is the carbon atom C13. Oxygen atom O1 and carbon atom C13 are susceptible to electrophilic and nucleophilic attack respectively for compound LESS4. The O3 atom has the highest nucleophilic Fukui number for the population analysis used when C13 has the highest electrophilic Fukui number. Consequently, any electrophilic attack will be made on the O3 atom when a nucleophilic attack will be made on the C13 atom concerning LESS5.

This first part of our study on the influence of linker shortening on reactivity showed that when we shorten the linker, the center of reactivity changes completely from O15 for electrophilic attacks on O3 and from O3 for nucleophilic attacks on C13. Oxygen O1 often appears regardless of whether it's the nucleophilic site.

Table 7: Local reactivity index values for MORE derivatives of SAHA

		O_1	N_2	O_3	C_4	O_{15}	C_{13}	N_{12}
MORE 1	f_k^+	0.028	0.018	0.053	0.075	0.075	0.103	-0.010
	f_k^-	0.104	0.078	0.070	0.003	0.074	0.000	0.089
	f_k^0	0.066	0.048	0.067	0.039	0.074	0.052	0.039
MORE 2		O_1	N_2	O_3	C_4	O_{15}	C_{13}	N_{12}
	f_k^+	0.058	0.065	0.061	0.103	0.068	0.115	0.016
	f_k^-	0.023	0.054	0.119	-0.001	0.080	0.000	0.097
	f_k^0	0.041	0.059	0.090	0.051	0.074	0.057	0.057
MORE 3		O_1	N_2	O_3	C_4	O_{15}	C_{13}	N_{12}
	f_k^+	0.031	0.029	0.058	0.071	0.072	0.100	-0.010
	f_k^-	0.024	0.047	0.134	0.001	0.076	0.000	0.093
	f_k^0	0.027	0.038	0.096	0.036	0.074	0.050	0.041
MORE 4		O_1	N_2	O_3	C_4	O_{15}	C_{13}	N_{12}
	f_k^+	0.015	0.033	0.080	0.121	0.056	0.090	0.008
	f_k^-	0.081	0.100	0.110	-1.172	0.072	-0.004	0.063
	f_k^0	0.048	0.067	0.095	-0.525	0.064	0.043	0.035
MORE 5		O_1	N_2	O_3	C_4	O_{15}	C_{13}	N_{12}
	f_k^+	0.027	0.018	0.055	0.080	0.072	0.101	-0.010
	f_k^-	0.105	0.081	0.071	0.003	0.073	0.000	0.088
	f_k^0	0.066	0.050	0.063	0.042	0.073	0.051	0.039

Analysis of the values in this table shows that oxygen O1 is more favorable for electrophilic attack. As far as nucleophilic attack is concerned, the C13 carbon atom will be the most favored in the MORE 1 compound, unlike SAHA, which has the O15 oxygen atom as the nucleophilic site and O1 as the electrophilic site. For MORE 2, the O3 atom has the highest nucleophilic Fukui number for the population analysis used, while C13 has the highest electrophilic Fukui number. Consequently, any electrophilic attack will be on the O3 atom when a nucleophilic attack will be on the C13 atom. But the atoms of particular interest for the study of SAHA always remain different for these derivatives.

The oxygen atom O3 is the most preferred site for electrophilic attack in the MORE3 compound, while the carbon atom C13 is designated as the nucleophilic attack site. Unlike SAHA, which predicts the oxygen atom O15 as the nucleophilic site and O1 as the electrophilic site. Local descriptor values for MORE4 show that carbon C4 is both the nucleophilic and electrophilic attack site. SAHA, on the other hand, sets its nucleophilic and electrophilic sites at oxygen O15 and O3 respectively. Indications for MORE4 show that oxygen O1 is the most favorable for electrophilic attack. As far as nucleophilic attack is concerned, the C13 carbon atom is the most favored. This is in contrast to the atoms predicted by SAHA as nucleophilic and electrophilic sites.

Overall, the local Fukui indices of the eleven (11) compounds, indicate oxygen O1 as the most nucleophilic preferred for electrophilic attack in general and carbon C13 as the most nucleophilic attack site. Often, however, oxygen O3 is indicated as the most nucleophilic.

HDAC1 model descriptors and predicted inhibitory activities

In this study, we used the model of Soro et al [13] to determine the inhibition concentration. Three geometric descriptors were exploited, namely the carbon-oxygen distance, the angles α°(O=C-N) and α°(H-N=O) found within the core of suberoylanilide hydroxamic acid (SAHA) derivatives. The values are shown in the following table :

Table 8: Descriptor values and theoretical inhibitory activity of the HDAC1 model of SAHA derivatives.

Compounds	d(C=O)(Å)	α (O=C-N)(°)	α (H-N-O) (°)	IC(théo) (µM)
LESS0	1.233	122.795	115.871	-15.778
LESS1	1.226	121.575	113.631	3.908
LESS2	1.228	119.900	111.673	-7.323
LESS3	1.214	119.229	111.536	100.067
LESS4	1.226	119.753	111.286	-4.690
LESS5	1.214	118.938	111.386	103.770
MORE1	1.226	119.671	111.018	-4.610
MORE2	1.214	119.031	111.025	94.952
MORE3	1.214	118.859	111.320	104.159
MORE4	1.258	120.007	109.472	-278.102
MORE5	1.226	119.646	110.997	-4.436

This HDAC1 model shows negative inhibition concentration values for compounds LESS0, LESS2, LESS4, MORE1, MORE4 and MORE5. These negative values confirm that these compounds are not active on HDAC1. Compounds LESS1, LESS3, LESS5, MORE2 and MORE3 are active, as they show positive inhibition concentrations. However, the study carried out by Yao et al [8] in 2014 shows that SAHA has an inhibition concentration of 0.131µM. This means that all these compounds have an inhibition concentration well above that of SAHA. Linker variation does not positively influence the inhibition concentration of suberoylanilide hydroxamic acid on HDAC1.

Descriptors and inhibition potential of the HDAC7 model

This model, developed by Soro et al [13] in 2018, requires a number of descriptors that we have identified after optimization and frequency calculation. These descriptors are the vibrational frequencies V(O-H) and V(N-H) and the electronic affinity. The values are shown in the following table :

Table 9: Theoretical inhibition potential descriptors for the HDAC7 model of SAHA derivatives

Compounds	$\mathbf{V(N-H)}(cm^{-1})$	$\mathbf{V(O-H)}(cm^{-1}$	A-E(eV)	pIC(théo)	IC50(µM)
LESS0	3657.5300	3623.3000	-0.0839	26.3351	0.0000
LESS1	3528.3000	3609.9700	-0.5881	34.6376	0.0000
LESS2	3634.0700	3581.9300	-0.9203	14.9440	**0.0011**
LESS3	3546.7400	3779.4200	-0.8436	93.0619	0.0000
LESS4	3624.7200	3575.9000	-0.9165	13.7070	0.0196
LESS5	3544.0800	3784.9700	-0.8856	95.3285	0.0000
MORE1	3618.5900	3576.0600	-0.8770	14.3068	0.0049
MORE2	3541.7400	3787.4000	-7.3700	103.9871	0.0000
MORE3	3544.4200	3785.5400	-0.8275	95.4296	0.0000
MORE4	3670.9700	3854.0000	-2.0068	108.8392	0.0000
MORE5	3618.1700	3575.3600	-0.8223	14.0359	0.0092

Analysis of the table shows the inhibition potential and inhibition concentration values. Inhibition concentrations were calculated using the relationship: **$pIC(théo)=-\log(IC_{50}.10^{-6})$.** At the 10-4 order, several compounds have insignificant concentrations, such as: LESS0, LESS1, LESS3, LESS5, MORE2, MORE3 and MORE4. These compounds will therefore be inactive in the fight against cancer cells. In addition, other molecules such as LESS1, LESS4, MORE1 and MORE5 show interesting inhibition concentrations. These values range from 0.0011 to 0.0192 µM. The compound LESS2, with the lowest concentration value, is the most active. However, a study by Yiwu Yao et al [8] in 2014 showed that SAHA had a concentration of 38.9 µM. Compared with SAHA, the LESS2 molecule has better inhibitory activity.

IV. CONCLUSION

The main aim of this work was to evaluate the reactivity and predict the biological activities of certain vorinostat (SAHA) derivatives. We varied the bond length to obtain eleven (11) compounds, which were studied using the DFT method. Calculations were performed at the theoretical level B3LYP/6-311G (d, p). The analysis showed that these new compounds can be formed at room temperature. The exploitation of global and local reactivity indices identified the sp3-hybridized O1 and sp2-hybridized O3 oxygens, belonging to the hydroxamic function, as the most favorable sites for electrophilic attack. For these compounds, these carbon atoms are the binding sites for zinc contained in cancer cells. As regards the prediction of the biological activities of these compounds, the HDAC1 model predicts for all these compounds a mediocre biological activity compared with that of SAHA. However, using the data obtained from the HDAC7 model, only LESS2 showed better inhibitory activity than SAHA. It is therefore clear that the biological activity of these compounds does not depend on carbon chain length. Based on these results, we are now in a position to envisage a metal-ligand study of these compounds.

BIBLIOGRAPHICAL REFERENCES

[1]. O. Witt, H. E. Deubzer, T. Milde Et I. Oehme, «Hdac Family: What Are The Cancer Relevant Targets?,» Cancer Lett., Vol. 277, N° %11, Pp. 8-21, 2009.

[2]. M. Haberland, R. L. Montgomery Et E. N. Olson, «The Many Roles Of Histone Deacetylases In Development And Physiology: Implications For Disease And Therapy,» Nat. Rev. Genet., Vol. 10, N° %11, P. 32–42, 2009.

A. Grabarska Et J. Luszczki, «Histone Deacetylase Inhibitor Saha As Potential Targeted Therapy Agent For Larynx Cancer Cells,» J. Cancer, Vol. 8, N° %11, Pp. 19-28, 2017.

[3]. M. Arnold, D. Brown, O. Deeg, W. Errington, W. Haase, K. Herlihy, T. J. Kemp, H. Nimir Et R. Werner, «Hydroxamate-Bridged Dinuclear Nickel Complexes As Models For Urease Inhibition,» Inorg. Chem, Vol. 1669, N° %15, P. 2920–2925, 1998.

[4]. M. Tegoni, F. Dallavalle Et M. Amélia Santos, «Succinylhydroxamic Derivatives Of Alpha-Amino Acids As Mmp Inhibitors. Study Of Complex-Formation Equilibria With Cu2+, Ni2+ And Zn2+,» J. Inorg. Biochem., Vol. 98, N° %12, P. 209–218, 2004.

A. Mogal Et S. A. Abdulkadir, «Effects Of Histone Deacetylase Inhibitor (Hdaci); Trichostatin-A (Tsa) On The Expression Of Housekeeping Genes,» Mol. Cell. Probes, Vol. 20, P. 81–86, 2006.

[5]. F. Muri, M. Nieto, R. D. Sindelar Et J. S. Williamson, «Hydroxamic Acids As Pharmacological Agents,» Curr. Med. Chem., Vol. 9, N° %117, P. 1631–1653, 2002.

[6]. Y. Yao, C. Liao, Z. Li, Z. Wang, Q. Sun, S. J. Yang Et Z. Tu, «Synthesis , And Biological Evaluation Of 1 , 3-Disubstituted- Pyrazole Derivatives As New Class I And Iib Histone Deadeacetylase Inhibitors,» Eur. J. Med. Chem., Vol. 86, N° %12, P. 639–652, 2014.

[7]. K. P. Holland, H. L. Elford, V. Bracchi, C. G. Annis, S. M. Schuster Et D. Chakrabarti, «Antimalarial Activities Of Polyhydroxyphenyl And Hydroxamic Acid Derivatives,» Antimicrob. Agents Chemother, Vol. 42, N° %19, P. 2456–2468, 1998.

[8]. M. J. Miller, «Syntheses And Therapeutic Potential Of Hydroxamic Acid Based Siderophores And Analogs,» Chem. Rev., Vol. 89, N° %17, P. 1563–1579, 1989. .

[9]. J. El Yazal Et Y.-P. Pang, «Novel Stable Configurations And Tautomers Of The Neutral And Deprotonated Hydroxamic Acids Predicted From High-Level Ab Initio Calculations,» J. Phys. Chem. A, Vol. 103, N° %141, P. 8346–8350, 1999.

A. Min, S. Im, D. Kim, S. Song, H. Kim, K. Lee, T. Kim, S. Han, D. Oh Et J. Bang, «Histone Deacetylase Inhibitor, Suberoylanilide Hydroxamic Acid (Saha), Enhances Anti-Tumor Effects Of The Poly (Adp-Ribose) Polymerase (Parp) Inhibitor Olaparib In Triple-Negative Breast Cancer Cells,» Breast Cancer Res., Vol. 17, P. 33, 2015.

[10]. D. Soro, L. Ekou, M. G.-R. Koné, T. Ekou, S. T. Affi, L. Ouattara Et N. And Ziao, «Prediction Of The Inhibitory Concentration Of Hydroxamic Acids By Dft-Qsar Models On Histone Deacetylase 1,» International Research Journal Of Pure & Applied Chemistry, Vol. 16, N° %12, Pp. 1-13, 2018.

[11]. M. J. Frisch, G. W. Trucks, H. B. Schlegel Et G. E. Scuseria, «Gaussian 09, Revision A.02,» Gaussian, Inc., Wallingford Ct, 2009.

[12]. Roy Dennington, Todd A. Keith, And John M. Milliam, «Gaussview, Version 6,» Semichem Inc. Shawnee Mission Ks, 2016.

[13]. O. V. Dorofeeva, V. P. Novikov Et D. B. Neumann, «Nist-Janaf Thermochemical Tables. I. Ten Organic Molecules Related To Atmospheric Chemistry,» Journal Of Physical And Chemical , Vol. 30, N° %12, P. 475–513, 2001.

[14]. T. Koopmans, «By Assigning Wave Functions And Values For The Individual Electron One Atom,» Physica, Vol. 1, P. 104, 1934.

[15]. N. T. Tuo, B. Ouattara, M. G. R. Kone, G. S. Dembele, D. Soro, F. Konate Et N. Ziao, «Theoretical Study Of Reactivity And Stability Of A Thiazoline Derivative Series By The Density Functional Theory Method.,» American Journal Of Applied Chemistry, Vol. 10, N° %15, Pp. 156-163., 2022.

[16]. N. Tuo, G. Dembele, D. Soro, F. Konate, B. Konate, C. Kodjo Et N. Ziao, «Theoretical Study Of The Chemical Reactivity Of A Series Of 2, 3-Dihydro-1h-Perimidine,» International Research Journal Of Pure & Applied Chemistry, Vol. 23, N° %11, Pp. 13-25, 2022.

[17]. P. W. Ayers Et R. G. Parr, «Variational Principles For Describing Chemical Reactions: The Fukui Function And Chemical Hardness Revisited,» J. Am. Chem. Soc., Vol. 122, N° %19, P. 2010–2018, Mars 2000.

[18]. W. Yang Et R. G. Parr, «Hardness, Softness, And The Fukui Function In The Electronic Theory Of Metals And Catalysis,» Proc. Nat Usa, Vol. 82, P. 6723, 1985.